Forward Electron Transfer from Phylloquinone A_1 to Iron–Sulfur Centers in Spinach Photosystem I†

Pierre Sétif*,‡ and Klaus Brettel*,§,∥

Section de Bioénergétique-CNRS, URA 1290, Département de Biologie Cellulaire et Moléculaire, C.E. Saclay, 91191 Gif sur Yvette, Cedex, France, and Max-Volmer-Institut für Biophysikalische und Physikalische Chemie, Technische Universität Berlin, Strasse des 17. Juni 135, 1000 Berlin 12, Germany

Received February 10, 1993; Revised Manuscript Received April 28, 1993

ABSTRACT: Forward electron transfer at room temperature from the secondary acceptor A_1 (phylloquinone) to the iron–sulfur centers F_X, F_B, and F_A was studied by flash-absorbance spectroscopy in different photosystem I (PSI) preparations in order to resolve the controversy concerning the kinetics of A_1^- reoxidation during forward electron transfer [half times of 15 ns [Mathis, P., & Sétif, P. (1988) *FEBS Lett. 237*, 65–68] and 200 ns [Brettel, K. (1988) *FEBS Lett. 239*, 93–98] were reported for PSI particles from spinach and *Synechococcus* sp., respectively]. The monophasic kinetics with $t_{1/2} \approx 200$ ns could be reproduced with PSI particles from another cyanobacterium (*Synechocystis* sp. PCC 6803). In so-called PSI-β particles from spinach, containing all membrane-bound electron carriers and approximately 65 antenna chlorophylls per reaction center, the flash-induced absorbance increase around 370 nm, which is indicative of the formation of A_1^-, decays biphasically with $t_{1/2} \approx 25$ and 150 ns and relative amplitudes of approximately 65 and 35%, respectively. The difference spectra of these two phases were determined between 330 and 500 nm; they agree well below 380 nm but deviate significantly at higher wavelengths. The spectrum of the sum of the two phases is similar to the spectrum of the 200-ns phase in cyanobacteria. Upon chemical reduction of the terminal acceptors F_A and F_B, only the 25-ns phase is conserved and the absorbance changes remaining after its completion decay with $t_{1/2} \approx 250$ μs. It is concluded that the 25-ns phase reflects electron transfer from A_1^- to F_X in approximately 65% of the centers, whereas the remaining 35% of A_1^- is reoxidized with $t_{1/2} \approx 150$ ns under moderate redox conditions. The deviations between the spectra of the two phases can be explained with the assumption that electron transfer from F_X^- to (F_A,F_B) also proceeds with $t_{1/2} \approx 150$ ns and contributes significantly to the total spectrum of the 150-ns phase, implying that the F_X^-/F_X difference spectrum deviates from the $(F_A,F_B)^-/(F_A,F_B)$ spectrum. Possible kinetic schemes for forward electron transfer in PSI-β particles are discussed; assuming that the 25-ns phase reflects the establishment of a redox equilibrium between reduced A_1 and F_X, the redox potentials of A_1 and F_X are found to be very close. Different types of PSI particles from spinach, which were subjected to less harsh preparation procedures, also exhibit a biphasic reoxidation of A_1^- but smaller relative amplitudes of the 25-ns phase, down to only 30% for a sample prepared without detergent. It is suggested that PSI in native spinach membranes could behave similarly to the cyanobacterial PSI particles.

Light excitation of photosystem I (PSI)[1] reaction centers induces a charge separation between the primary donor P700 (a dimer of chlorophyll *a* molecules) and a series of electron acceptors. The electron-transfer (ET) pathway within these acceptors is still far from being fully understood. Among the specific characteristics of this photosystem which have up to now prevented a more complete understanding, one can cite (1) the very low redox potentials of the PSI electron acceptors, which makes redox manipulation difficult; (2) the large number of these electron acceptors; and (3) the fact that three of these acceptors are iron–sulfur centers and are not easily distinguishable by spectroscopic methods at room temperature. Five PSI acceptors have been identified at the moment, from the primary acceptor, a chlorophyll molecule named A_0, to the terminal membrane-bound ferredoxin, which is similar to the 2[4Fe-4S] bacterial ferredoxin [see Golbeck and Bryant (1991) for a review]. This terminal ferredoxin carries two [4Fe-4S] clusters, which are named F_A and F_B, which up to now have appeared to be indistinguishable by flash-absorbance spectroscopy. Two other acceptors, named A_1 and F_X, are generally thought to mediate the electron transfer from the primary acceptor to the terminal iron–sulfur centers. The identification of the chemical nature of these two acceptors has recently been a major field of investigation in PSI research. It is now widely accepted that A_1 is a molecule of phylloquinone (vitamin K_1) [see Golbeck and Bryant (1991) for a review and the references in Rustandi et al. (1992) for more recent work], whereas recent studies provide evidence that F_X is a [4Fe-4S] cluster (Petrouleas et al, 1989; McDermott et al., 1989).

With respect to the ET pathway to the iron–sulfur centers F_A, F_B, and F_X, both parallel and linear electron-transfer schemes have been proposed (see, e.g., Rutherford and Heathcote (1984) for a review]. All these schemes were based on experiments at low temperature (where the three centers can be distinguished by EPR), but few data are available concerning the kinetics of reduction of these centers during forward electron transfer at room temperature. Secondary

† This work was supported by an EMBO fellowship (P.S.) and by grants from the Deutsche Forschungsgemeinshaft (Sonderforschungsbereich 312, Teilprojekt A3 and A5) (K.B.).

‡ Section de Bioénergétique-CNRS.

§ Max-Volmer-Institut für Biophysikalische und Physikalische Chemie.

∥ Present address: Section de Bioénergétique-CNRS, URA 1290, Département de Biologie Cellulaire et Moléculaire, C.E. Saclay, 91191 Gif sur Yvette, Cedex, France.

[1] Abbreviations: PSI, photosystem I; ET, electron transfer; Fe-S, iron–sulfur center; F_A, F_B, and F_X, the [4Fe-4S] centers of photosystem I; EPR, electron paramagnetic resonance.

0006-2960/93/0432-7846$04.00/0

ET reactions, which presumably involve A_1, have been identified only recently through the use of time-resolved absorbance and EPR spectroscopies. The reoxidation of A_0^- has been found to occur within 30–200 ps [see Sétif (1992) for a review]. From these picosecond absorbance studies, the species oxidizing A_0^- has not been identified but is most probably A_1. This last attribution can be made on the basis of experiments involving the extraction of phylloquinone and its reinsertion into the reaction center (Biggins & Mathis, 1988; Itoh & Iwaki, 1989) and of studies presumably involving the double reduction of A_1 (Sétif & Bottin, 1989); it is also in line with absorbance studies with a nanosecond time resolution indicating that A_1 is reduced within less than 5 ns (Brettel, 1988).

Recently, kinetic phases of 15 ns (Mathis & Sétif, 1988) and 200 ns (Brettel, 1988) were observed respectively in spinach and cyanobacterial PSI particles by flash-absorbance spectroscopy at room temperature. The 15-ns phase in spinach PSI was assigned to ET from A_1^- to F_X because of its insensitivity to chemical prereduction of both F_A and F_B. The 200-ns phase in cyanobacterial PSI was characterized by its absorbance difference spectrum in the UV and blue regions and by spin-polarized EPR spectra obtained by time-resolved EPR spectroscopy (Bock et al., 1989). Both data sets were compatible with ET from A_1^- (phylloquinone) to an iron–sulfur center (F_X, F_A, or F_B). As chemical prereduction of both F_A and F_B blocked the 200-ns forward ET (Brettel, 1989), it was even speculated that A_1^- might transfer its electron directly to F_A and/or F_B, without involving F_X.

We have now reinvestigated the ET reactions involving A_1^- in spinach PSI by flash-absorbance spectroscopy with an improved signal-to-noise ratio and a largely extended spectral range. It is shown that the conflicting previous results were due to a large extent to the use of different biological materials and that reoxidation of A_1^- in spinach PSI particles is in fact biphasic with half times of 25 and 150 ns. The presence of these two phases, their differential sensitivity to the prereduction of both F_A and F_B, and the comparison with flash-absorbance signals due to recombination reactions under different redox conditions allow us to give a better description of the forward electron-transfer steps in PSI.

EXPERIMENTAL PROCEDURES

Biological Samples. Different types of detergent PSI particles from spinach were prepared according to Vernon (1971) (Triton particles named TSF1), Boardman (1971) (digitonin particles named D144), Picaud et al. (1982) (digitonin–deoxycholate particles named PSI-110), and Lagoutte et al. (1984) (PSI-β particles). Most of the experiments described in the present paper involve PSI-β particles. These particles were prepared basically as the PSI-110 particles, except that solubilization by digitonin was preceded by overnight incubation of the thylakoid membranes in the presence of 5% β-mercaptoethanol at pH 8.8. They contain about 65 chlorophylls per P700. TSF1, D144, and PSI-110 particles contain respectively about 200–250, 200–250, and 110 chlorophylls per P700. A sample of a nondetergent PSI preparation from spinach was kindly provided by Dr. P. Bogdanoff. In brief, class II chloroplasts were suspended at 2×10^{-4} M chlorophyll in a buffer containing 50 mM NaH_2PO_4/NaOH (pH 7.4) and 150 mM NaCl and passed twice through a YEDA press at 10 MPa. After a 30-min centrifugation at 40000g, the supernatant contained membrane fragments enriched in PSI (PSI/PSII $\approx$ 40). They were pelleted by a 30-min centrifugation at 100000g, resuspended in a buffer containing 5 mM NaH_2PO_4/NaOH (pH 7.4), 2 mM $MgCl_2$, 400 mM saccharose, and 5% (v/v) DMSO, and stored in liquid nitrogen until used. PSI particles from *Synechocystis* sp. PCC 6803 were prepared as described by Bottin and Sétif (1991). They contain about 110 chlorophylls per P700. Unless otherwise stated, the particles were suspended in 50 mM Tris·HCl at pH 8.

Spectroscopic Measurements. Flash-induced absorbance measurements with a time resolution of 5 ns were performed with the setup described by Gerken et al. (1987), using repetitive excitation (1.7 Hz) by 532-nm laser flashes of 3-ns duration, approximately 2 mJ/cm^2. The bandwidth (full width at half-maximum) of the measuring beam was usually between 7 and 10 nm, except for measurements at 450 and 488 nm where it was only 3 nm. Flash-induced absorbance measurements with a time resolution of 30 μs were performed as described by Brettel (1988). Measurements under highly reducing conditions were performed with a nanosecond time resolution at only two different wavelengths, 371 and 475 nm. For each measurement, a fresh sample was used. The absorbance changes were measured first at 700 nm with a time resolution of 30 μs and then at a given wavelength with a 5-ns time resolution ($\leq$512 laser flashes) and were checked again at 700 nm with 30-μs time resolution. Absorbance changes were also recorded at all wavelengths in the presence of potassium ferricyanide (P700 initially oxidized). The signals thus obtained were very small and were not subtracted from the signals obtained under moderate or highly reducing conditions. All experiments were done at room temperature. Decay curves were fitted to a multiexponential decay using a Marquardt least-squares algorithm.

RESULTS

Electron Transfer under Moderate Redox Conditions. Figure 1 shows typical examples of the absorbance change kinetics following flash excitation of PSI-β particles from spinach under moderate redox conditions. Such measurements were performed at 19 different wavelengths between 330 and 500 nm and will be analyzed as follows. The "initial" (5 ns after the flash excitation) and "final" (1.6 μs after the flash) absorbance changes are plotted as a function of wavelength in Figure 2 as crosses and squares, respectively. These spectra are very similar to the corresponding spectra observed previously in PSI particles from the cyanobacterium *Synechococcus* sp. [see Figure 4 in Brettel (1988)], except for smaller positive absorbance changes around 450 nm (see Discussion). As it was previously proposed (Brettel, 1988), these two spectra can be ascribed respectively to the states ($P700^+$–A_1^-) and ($P700^+$–Fe-S^-), Fe-S being one of the three iron–sulfur centers present in PSI. Whereas the latter spectrum agrees well with the sum of the difference spectra for P700 oxidation and for the one-electron reduction of (F_A,F_B) published by Ke (1972), the attribution of the former spectrum was based (1) on the large positive signals observed from 340 to 400 nm, which agree with the spectrum for ($P700^+$–A_1^-) formation observed at 10 K (Brettel et al., 1986) and are consistent with the known spectrum for the one-electron reduction of vitamin K_1; and (2) on the observation of an EPR signal, with a similar kinetic behavior, which has been ascribed to the weakly coupled radical pair ($P700^+$–A_1^-) (Bock et al., 1989).

Examination of the transition between the initial and final spectra presented in Figure 2 reveals that at least two exponential phases are required to fit this transition throughout the wavelength range studied: a phase with a half time of

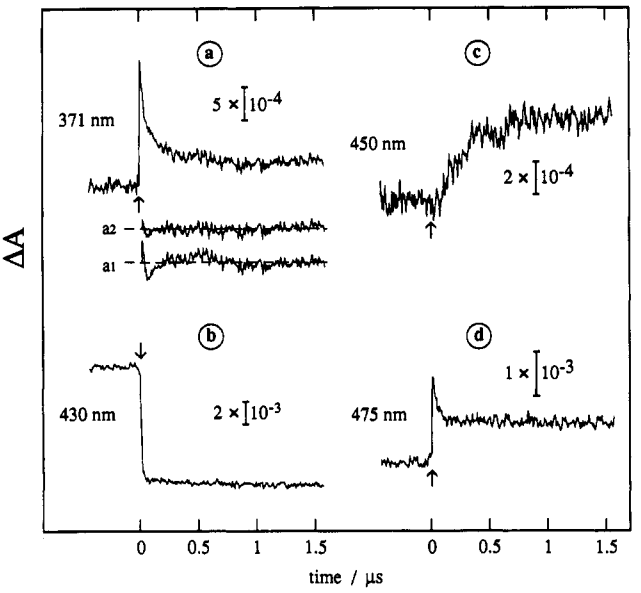

FIGURE 1: Flash-induced absorbance changes measured in PSI-β particles from spinach under moderate redox conditions at 371 nm (trace a), 430 nm (trace b), 450 nm (trace c), and 475 nm (trace d). The PSI particles (absorbance at 678 nm = 0.98) were suspended in 50 mM Tris·HCl, pH 8, in the presence of 1 mM sodium ascorbate, 120 μM 2,6-dichlorophenolindophenol, and 60 μM methyl viologen. Traces are averages of 128 (trace b), 256 (trace d), and 512 (traces a and c) experiments. Traces a1 and a2 are the residuals of one- and two-exponential fits, respectively, to the signal at 371 nm. For both fits, an offset parameter was used in addition to the exponential phases in order to take into account some longer-lived absorbance changes. The fit with one exponential (residual a1) yielded 79% of a phase with $t_{1/2}$ = 84 ns and 21% of offset. The two-exponential fit (residual a2) was performed with fixed half times of 25 and 150 ns and yielded 56% of the 25-ns phase, 30% of the 150-ns phase, and 15% of offset.

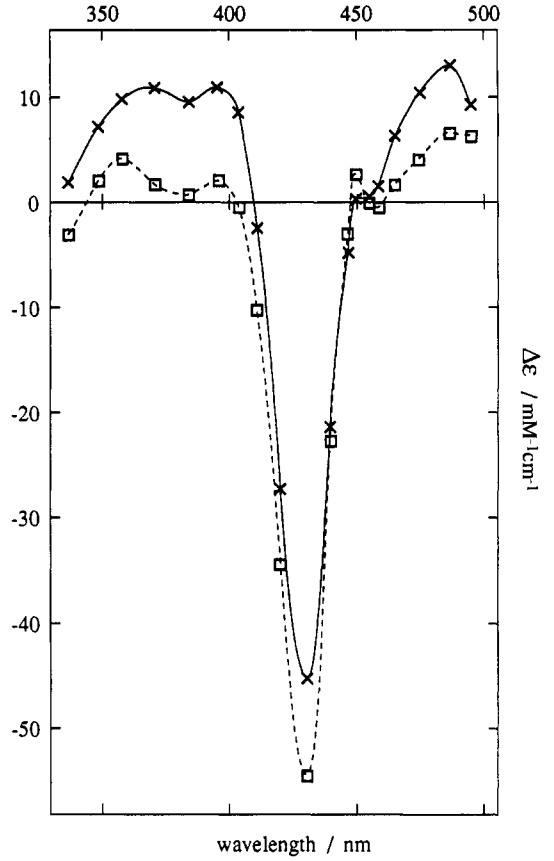

FIGURE 2: Spectra of the flash-induced absorbance changes measured in PSI-β particles between 330 and 500 nm at approximately 5 ns (crosses) and 1.6 μs (squares) after excitation (taken from measurements as those depicted in Figure 1). The vertical scale was calibrated assuming a $\Delta\epsilon$ of 54 500 M^{-1} cm^{-1} for the signal at 430 nm and at 1.6 μs after the flash. This value corresponds to the sum of the $\Delta\epsilon$ values for the oxidation of P700 and for the one-electron reduction of (F_A,F_B) given by Ke (1972) at this wavelength.

approximately 25 ns, which is close to the value of 15 ns reported previously for the same material (Mathis & Sétif, 1988), and a phase with a half time of approximately 150 ns, which is close to the value of 200 ns reported for PSI from *Synechococcus* (Brettel, 1988). The relative sizes of these two components vary from one wavelength to another (see kinetics in Figure 1); at 371 nm (Figure 1, trace a), the two components are positive, with the amplitude of the faster component being roughly twice that of the slower one. This explains why only a fast component was observed at this wavelength in a previous study where the signal-to-noise ratio was smaller (Mathis & Sétif, 1988). Traces a1 and a2 in Figure 1 show the residuals from the data fits with 1 and 2 exponentials, respectively (for details, see the caption of Figure 1), demonstrating that at least two exponential phases are required to obtain an acceptable fit at 371 nm. At some particular wavelengths, one of the two components appears negligible compared to the other one. This can be seen for example at 475 nm (Figure 1, trace d; mostly faster component) and at 450 nm (Figure 1, trace c; mostly slower component). At 430 nm (Figure 1, trace b), the strong bleaching due to P700 oxidation dominates the absorbance change.

At each wavelength, the transient signal was analyzed, assuming the presence of two exponential components with fixed half times of 25 and 150 ns. The magnitude of both components was thus calculated at each wavelength, and the resulting spectra are plotted in Figure 3. It should be noted that we regard the data between 420 and 440 nm as not reliable because of the largely dominating bleaching due to the oxidation of P700. Therefore, the lines connecting the data points are interrupted in this region. First, we consider the spectrum of the sum of the 25- and 150-ns components (top panel of Figure 3, crosses and solid line). This spectrum resembles the spectrum of the 200-ns component observed under similar conditions in PSI particles from *Synechococcus* sp. (Figure 3, dashed line in top panel) which was ascribed to electron transfer from A_1^- to an iron–sulfur center. However, a significant difference should be noted: the negative peak is blue shifted from 458 nm in *Synechococcus* to 450 nm in PSI-β from spinach and is less pronounced in the latter material. The spectrum of the 25-ns phase (middle panel of Figure 3) has an overall shape similar to that of the sum of both phases, but it remains positive even around 450 nm. The shape of the 150-ns phase spectrum (bottom panel of Figure 3) is rather different from the spectrum of the 25-ns phase except for the region below 380 nm. Omitting the 420–440-nm range and considering that the relative uncertainty is larger for a component with smaller amplitude, there remain three significant deviations between the spectra of the 25- and 150-ns phases: (a) the 150-ns phase is negative around 450 nm, whereas the 25-ns phase is slightly positive (see also trace c in Figure 1); (b) the 150-ns phase is negligible or even negative between 460 and 500 nm, where the 25-ns phase has relatively large positive amplitudes (see also trace d in Figure 1); (c) the spectrum of the 150-ns phase has a trough around 400 nm, where the 25-ns phase has a maximum. The significantly different shapes of the two spectra provide evidence that the 25- and 150-ns phases represent different reactions and not just a heterogeneity in the rate of one and the same electron-transfer step (see Discussion).

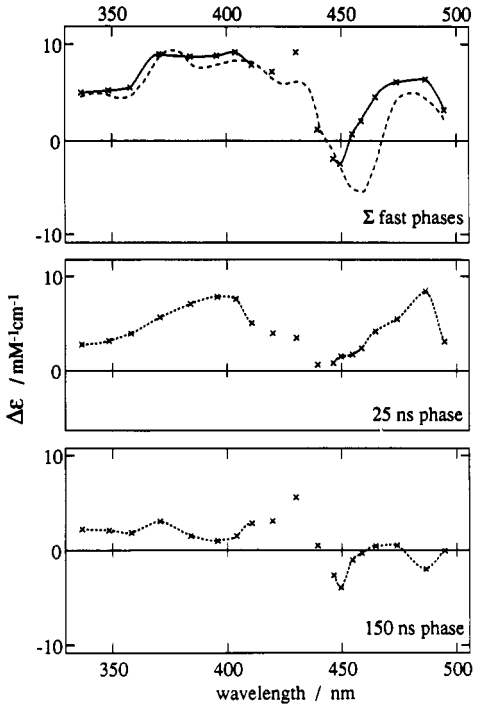

FIGURE 3: Spectra of the 25-ns (middle panel) and 150-ns phases (bottom panel) and of the sum of both phases (top panel, crosses and solid line) resulting from the analysis into two exponential phases of the submicrosecond kinetics measured in PSI-β particles (see text for further details). These spectra are extracted from measurements like those depicted in Figure 1. The $\Delta\epsilon$ scale was calibrated as in Figure 2. The dashed line shown in the top panel represents the spectrum of the 200-ns phase which was previously measured in PSI particles from *Synechococcus* (Brettel, 1988); this spectrum was recalibrated according to the procedure used for the other spectra.

Some data were also collected for PSI particles prepared from the cyanobacterium *Synechocystis* 6803. The results are virtually identical, in both their kinetic and spectral characteristics, with the results obtained previously for *Synechococcus* sp., where a single 200-ns phase has been observed (Brettel, 1988).

As the kinetic behavior of spinach PSI-β particles is very different from that of cyanobacterial PSI, it can be asked whether this could be due to the harsher treatment necessary for preparing these spinach particles. Therefore, the transient kinetics at 371 and 430 nm of different spinach PSI preparations were studied. In all preparations tested so far, the nanosecond kinetic behavior at 371 nm appears to be biphasic. This was checked for PSI particles prepared after detergent solubilization of the membranes (D144, TSF1, and PSI-110; see Experimental Procedures) as well as for a nondetergent preparation of PSI (YEDA press; see Experimental Procedures). The proportions of the two decay phases were estimated in these different spinach PSI particles, assuming $t_{1/2}$ values of 25 and 150 ns for the two phases in all the spinach samples (Table I). Whereas the kinetic behavior of spinach PSI-β particles is strikingly different from that of cyanobacterial PSI, the behavior of the other spinach particles is intermediate between these two extreme cases, with the nondetergent PSI particles behaving more closely like cyanobacterial PSI, with only 30% of a fast 25-ns phase at 371 nm. As already mentioned, the absorbance change kinetics in cyanobacteria are essentially monophasic with $t_{1/2} \approx 200$ ns, but considering the signal-to-noise ratio of such experiments, it cannot be excluded that a component with $t_{1/2} \approx 25$ ns with a relative amplitude of at most 15% is present. Table I also shows the ratio of the initial signal sizes (measured at 5 ns after the laser flash excitation) at 430 and 371 nm, as this last wavelength can be taken as an index of the presence of reduced A_1. All these ratios are found close to a value of 5, thus indicating that, in any case, the initial state is most probably the state ($P700^+$–A_1^-).

Table I: Kinetic and Spectral Characteristics of Forward Electron Transfer in Different PSI Preparations under Moderate Redox Conditions

	rel proportions of the two phases of A_1^- reoxidation[a] (%)		ratio of the initial[b] signal sizes at 430 and 371 nm
	$t_{1/2}$ = 25 ns	$t_{1/2}$ = 150 ns	
spinach PSI-β	65 ± 5	35 ● 5	4.2 ± 0.5
spinach YEDA press[c]	30 ± 10	70 ± 10	4.6 ± 1
spinach TSF1	40 ± 10	60 ± 10	6.7 ± 1
spinach D144	40 ± 10	60 ± 10	6.0 ± 1
spinach PS1-110	50 ± 10	50 ± 10	5.5 ± 1
Synechococcus sp.	<15(?)	>85[d]	4.0 ● 0.5
Synechocystis 6803	<15(?)	>85[d]	4.3 ± 0.7

[a] Measured at 371 nm. [b] At 5 ns after the flash excitation. [c] Suspended in 20 mM tricine, pH 7.8. [d] $t_{1/2} \approx 200$ ns.

The kinetic data presented so far were restricted to the time range up to 1.6 μs after excitation because of the use of a xenon flash as measuring light source. In order to check for forward electron-transfer reactions beyond 1.6 μs, we performed measurements on a 4-ms time scale with continuous measuring light around 380, 430, and 450 nm. We used PSI-β particles under moderate redox conditions but in the absence of the artificial electron acceptor methyl viologen. At all wavelengths studied, the absorbance change was found to decay only slowly on a 4-ms time scale, as expected for a recombination reaction between $P700^+$ and $(F_A,F_B)^-$ with $t_{1/2} \approx 30$ ms (Ke, 1973). More importantly, the initial absorbance change was found to correspond to the absorbance change detected at 1.6 μs after the flash in nanosecond experiments, as shown in Figure 4 for 371 nm (trace c compared with trace a) and at 450 nm (trace e compared with trace c of Figure 1). Therefore, we have no evidence for any further absorbance change following the 150-ns phase which would correspond to a forward electron-transfer step.

Electron Transfer under Highly Reducing Conditions. The spinach PSI-β particles were also studied under conditions where both F_A and F_B are prereduced by addition of sodium dithionite at pH 10. In that case, a fast phase with $t_{1/2} \approx 25$ ns is still present at 371 nm (Figure 4, trace b), in agreement with previous observations (Mathis & Sétif, 1988), and it has approximately (within 25%) the same magnitude as under moderate redox conditions. However, the 150-ns phase is no longer detectable and appears to be replaced by a much longer lived component. The same experiment has been conducted at 475 nm (not shown), with similar results (25-ns phase still present with a similar size). During these measurements, caution was taken to maintain F_X oxidized through the entire experiment (see Experimental Procedures), as controlled by the unchanged size of the 250-μs phase at 700 nm. Accumulation of reduced F_X had to be avoided, because it leads to the appearance of a fast ($t_{1/2} \approx 250$ ns) recombination reaction between $P700^+$ and A_1^- forming the P700 triplet state (Sétif & Brettel, 1990). At 371 nm, this last process corresponds to an absorbance decrease, so that the disappearance of the 150-ns phase in trace b of Figure 4 cannot be due to a compensation effect between kinetics of similar half times and of opposite signs. In fact, we observed that further accumulation of flashes with the sample used for Figure 4, trace b, led to the appearance of a decaying 250-ns phase,

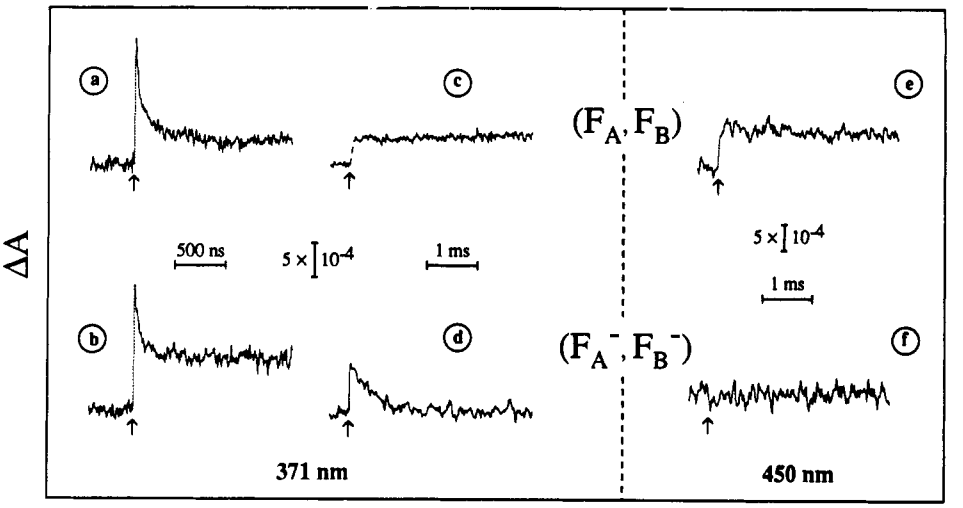

FIGURE 4: Flash-induced absorbance changes measured in PSI-β particles at 371 nm (left panel) and 450 nm (right panel) either under moderate redox conditions (upper traces) or under highly reducing conditions (lower traces; F_A and F_B prereduced). The full time scale of the measurements is 2 μs for the two leftmost traces (a and b) and 4 ms for the four rightmost. For the experiments under moderate redox conditions, the PSI particles were suspended as described in Figure 1, except that methyl viologen was omitted for traces c and e. For the experiments under highly reducing conditions, the PSI particles were suspended in 200 mM glycine/NaOH, pH 10, in the presence of 25 mM sodium dithionite. Traces are average of 512 (traces a and b) and 64 (traces c–f) experiments.

together with a decrease of the 25-ns phase at 371 nm and a decrease of the 250-μs phase at 700 nm (not shown). Because of these difficulties, the study of the nanosecond kinetics under conditions of prereduced F_A and F_B was not extended to other wavelengths. It was easier to study the 250-μs recombination reaction under conditions of prereduced F_A and F_B because fewer traces had to be averaged to get a sufficient signal-to-noise ratio. The 250-μs phase is generally thought to arise from a charge recombination between $P700^+$ and F_X^-, but more recently it has been demonstrated that a phase with the same half time in prereduced PSI particles from *Synechococcus* is due to recombination within the ($P700^+$–A_1^-) pair (Brettel, 1989). With prereduced PSI-β particles, we found that the initial absorbance changes decaying with a 250-μs half time exhibit a size which approximately corresponds to the size of the signal observed at the end of the 25-ns phase (at about 75 ns) under moderate redox conditions. This is shown for two different wavelengths, 371 and 450 nm (traces d and f of Figure 4 compared respectively with trace a of Figure 4 and with trace c of Figure 1). This has also been checked at 374, 454, and 459 nm (not shown). Thus comparison of both sets of data (spectra obtained during forward electron transfer and of the 250-μs recombination phase) suggests that the state of the reaction center which is the product of the 25-ns phase during forward electron transfer is similar to the state responsible for the 250-μs recombination reaction with prereduced F_A and F_B.

DISCUSSION

A strikingly different kinetic behavior was previously reported for PSI particles from spinach (Mathis & Sétif, 1988) and *Synechococcus* (Brettel, 1988). Our results extend considerably the study made on spinach particles by increasing the spectral range studied and improving the signal-to-noise ratio. It is confirmed that the flash-induced absorbance increase at around 370 nm, indicative of reduced A_1, decays clearly faster in the PSI-β preparation from spinach than in PSI from cyanobacteria. In fact, this decay turned out to be biphasic in the spinach preparation with half times of 25 and 150 ns representing approximately $^2/_3$ and $^1/_3$ of the total decay, respectively. The 150-ns phase had escaped detection in the previous study (Mathis & Sétif, 1988), probably because of the poorer signal-to-noise ratio. These results can be opposed to the observation of a single kinetic component with $t_{1/2} \approx$ 200 ns in PSI particles from *Synechococcus* (Brettel, 1988) and *Synechocystis*. The following discussion will first focus on the interpretation of the kinetic and spectral data of the PSI-β preparation from spinach which was studied most extensively and with a better signal-to-noise ratio in the present paper. Possible origins for the variation between different PSI preparations will be discussed subsequently.

When both F_A and F_B are prereduced in spinach PSI-β particles, the 150-ns phase disappears, whereas the fast phase is still observed. This fast phase exhibits characteristics of rate constant and magnitude which are similar, within a precision of 25%, to the fast phase observed under moderate redox conditions. As the positive amplitude of this phase around 370 nm indicates that it involves the oxidation of A_1^- and as F_X is the only available acceptor when both F_A and F_B are prereduced, we attribute the 25-ns phase to electron transfer from A_1 to F_X, in accordance with a previous interpretation (Mathis & Sétif, 1988). These results provide clear evidence for the participation of the iron–sulfur center F_X in forward ET at room temperature under conditions of moderate redox potential, at least in the PSI-β preparation from spinach. Such evidence could not be obtained for cyanobacterial PSI particles, where no forward electron transfer from A_1^- was detected after prereduction of F_A and F_B (Brettel, 1989). It may appear to the reader that the participation of F_X in normal forward electron transfer is obvious, as it has been known for a long time that this iron–sulfur center can be photoreduced. However, this cannot be viewed as a decisive argument, as in most cases, the yield of F_X reduction from the previous acceptors either was not measured or was found to be low [see, e.g., Sétif et al. (1984)]. Moreover, F_X photoreduction experiments were conducted under nonphysiological conditions: either at very low temperature (around 10 K), where the electron-transfer pathway may be considerably disturbed and quite different from the room temperature pathway (Sétif et al., 1987); after continuous illumination during freezing (Evans et al., 1975) when low-yield side paths of electron transfer are to be considered; or in core PSI lacking F_A and F_B (Golbeck & Cornelius, 1986), which could behave abnormally due to the biochemical pretreatments.

The 150-ns phase, which we have characterized by its absorbance difference spectrum (Figure 3, bottom) in the PSI-β preparation from spinach, is not easy to assign. One might suppose that this phase has the same origin as the 200-ns phase in the PSI preparations from cyanobacteria because of the similar half times and the similar behavior upon prereduction of both F_A and F_B. However, the difference spectrum of the 150-ns phase in PSI-β particles (Figure 3, bottom) is significantly different from that of the 200-ns phase in PSI particles from *Synechococcus* (Figure 3, top, dashed line). The spectrum of the 150-ns phase in PSI-β particles is also clearly different from that of the 25-ns phase in the same material (Figure 3, center), so it can be excluded that the two phases represent the same reaction with only different rates because of heterogeneity of the sample. Finally, the 150-ns phase might be assigned to ET from F_X to (F_A,F_B), also explaining most easily the disappearance of this phase upon prereduction of both F_A and F_B. However, two observations contradict this simple view: (1) The 150-ns phase exhibits a significant positive amplitude between 340 and 370 nm. In this region, ET between different [4Fe-4S] centers is not expected to give significant absorbance changes, as the differential extinction coefficient for the reduction of a given center is already very small [see, e.g., Ke (1972)]. The positive amplitudes of the 150-ns phase between 340 and 370 nm can be more easily explained by the assumption that some reoxidation of A_1^- is involved as well in this process. (2) A phase with $t_{1/2} \approx 150$ ns in the PSI-β preparation was also observed by transient EPR (A. J. van der Est, C. H. Bock, J. H. Golbeck, K. Brettel, P. Sétif, & D. Stehlik, in preparation). The spectral features of this phase are consistent with a transition from the spin-polarized pair ($P700^+$–A_1^-) to the spin-polarized pair ($P700^+$–Fe-S^-), with Fe-S being one of the three iron–sulfur centers. During the same experiments, the 25-ns phase could not be observed directly, as it is faster than the 50-ns time resolution of the EPR setup. However, the polarized spectrum observed after completion of the instrument-limited rise of the transients (i.e., at approximately 100 ns after flash excitation) is consistent with a superposition of the ($P700^+$–A_1^-) and ($P700^+$–Fe-S^-) spectra [see Bock et al. (1989)], with a large fraction of the sample being in the state ($P700^+$–Fe-S^-). This is presumably a result of the ET from A_1^- to F_X with $t_{1/2} \approx 25$ ns. These results suggest that the 150-ns phase observed in the PSI-β preparation by flash-absorbance spectroscopy involves some reoxidation of A_1^- concomitant with ET from F_X^- to (F_A,F_B). Assuming that ET between the iron–sulfur centers is silent in the 340–370-nm region, the relative amounts of A_1^- oxidation during the 25- and 150-ns phases under moderate redox conditions can be approximately calculated from the relative sizes of these two components between 340 and 370 nm: $(65 \pm 10)\%$ and $(35 \pm 10)\%$ of A_1^- is respectively oxidized during the 25- and 150-ns phases.

Summarizing, we favor the following assignment for the two phases: The 25-ns phase corresponds to electron transfer from A_1^- to F_X in 65% of the PSI-β centers. The 150-ns phase corresponds to reduction of (F_A,F_B), A_1^- and F_X^- being reoxidized in respectively 35% and 65% of the reaction centers during this step.

It should be pointed out that the significant differences between the spectra of the 25- and 150-ns components (Figure 3, center and bottom) necessarily imply that at least three states with different spectral properties are involved. Identifying the three states with ($P700^+$–A_1^-), ($P700^+$–F_X^-), and ($P700^+$–$(F_A,F_B)^-$), we can conclude that the difference spectrum for the reduction of F_X deviates significantly from that for the one-electron reduction of (F_A,F_B). Using the measured difference spectra and the assignment of the 25- and 150-ns phases given above, it can be inferred that reduction of F_X involves a stronger bleaching arround 400 nm, around 450 nm, and between 460 and 500 nm than reduction of (F_A,F_B).

The identity of the radical pair responsible for a recombination reaction with a half time of about 250 μs was recently a matter of debate. This decay phase, observed after prereduction of both F_A and F_B (Sauer et al., 1978), was generally ascribed to a recombination reaction between $P700^+$ and F_X^-, but has been shown recently to arise from a recombination between $P700^+$ and A_1^- in PSI particles from *Synechococcus* (Brettel, 1989). Our results on the PSI-β preparation from spinach indicate that the charge-separated state recombining with $t_{1/2} \approx 250$ μs under reducing conditions is similar to the state which is reached after completion of the 25-ns phase under moderate redox conditions, i.e., a superposition of ($P700^+$–F_X^-) and ($P700^+$–A_1^-), at a ratio of about 2:1.

The question arises whether the observed complexity of secondary ET in PSI is due to some heterogeneity in the sample or to a fast redox equilibrium between two species (A_1 and F_X) with similar redox potentials. In the former case, it could be assumed that about 35% of the spinach PSI-β centers behave similarly ($t_{1/2} \approx 150$ ns) to the cyanobacterial reaction centers, whereas 65% behave very differently, with a fast electron transfer with $t_{1/2} \approx 25$ ns between A_1 and F_X. The fact that we did not observe significant differences between the spectrum obtained at 1.6 μs after the flash in nanosecond experiments and the spectrum of the 30-ms phase attributed to the recombination between $P700^+$ and $(F_A,F_B)^-$ [although ET from F_X to (F_A,F_B) should be accompanied by absorbance changes (see above)] suggests that (F_A,F_B) is reduced 1.6 μs after the flash in all reaction centers. If this is the case, a second submicrosecond kinetic phase corresponding to the reduction of (F_A,F_B) should be present in those centers showing ET from A_1^- to F_X with $t_{1/2} \approx 25$ ns. This in turn could imply that the 150-ns phase is in fact composed of two different components due to each of the two subpopulations. This would also be compatible with the observation that the spectrum of the 150-ns phase in PSI-β particles deviates from the spectrum of the 200-ns phase in *Synechococcus*. Evidently our data can be accomodated by such a heterogeneity; as we will discuss in more detail in the following, our results on the PSI-β preparation can also be explained without introducing a heterogeneity if one assumes a fast redox equilibrium between A_1 and F_X.

A kinetic scheme involving such a redox equilibrium is depicted in Figure 5, top (model 1-2); models 1 and 2 (Figure 5, bottom) are borderline cases of the more general model 1-2. Model 1 assumes that (F_A,F_B) is reduced solely from F_X^- ($k_2 = 0$), whereas it is reduced solely from A_1^- in model 2 ($k_3 = 0$). For spinach PSI-β particles, several observations are to be accounted for in any model, i.e., half times of 25 and 150 ns and oxidation of A_1^- amounting to 65% and 35% for the fast and slow phases, respectively. In the case of model 1 or 2, a single set of rate constants (k_1, k_{-1}, k_2, and k_3) is found with the above constraints (Table II), whereas in the case of model 1-2, the solution is not unique, as there are more unknowns than equations to be satisfied. Any solution for this last model is limited by the solutions found for models 1 and 2, which constitute borderline cases of model 1-2. In other words, for any solution of model 1-2, the values of the four rate constants (k_1, k_{-1}, k_2, and k_3) are found between the

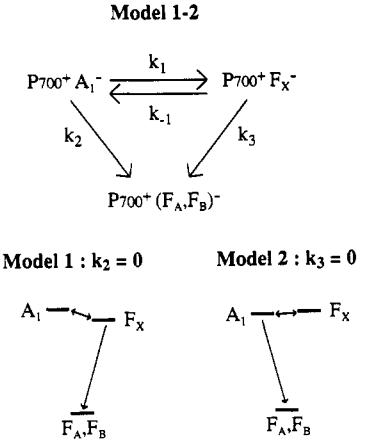

FIGURE 5: Models for the forward electron-transfer pathway in PSI involving the phylloquinone A_1 and the three iron–sulfur centers F_A, F_B, and F_X.

values calculated for models 1 and 2. A particular set for model 1-2 is given in the last line of Table II, assuming $k_2 = k_3$ (unique set with this additional constraint). Considering these different sets of rate constants, it was checked which of them are compatible with the measurements made under reducing conditions. Setting $k_2 = k_3 = 0$ under reducing conditions and using the same rate constants k_1 and k_{-1} as under normal conditions, we calculated the $t_{1/2}$ of the remaining fast phase and the percentage of A_1^- being reoxidized during this phase (Table II, last two columns). It turns out that the values predicted by model 1-2 with $k_2 = k_3$ are closest to the experimental result (no evident change of the half time and amplitude of the fast phase upon prereduction of both F_A and F_B), but according to the signal-to-noise ratio of those measurements, neither model 1 nor model 2 can be excluded. Furthermore, the assumption that k_1 and k_{-1} are not changed when F_A and F_B are prereduced may be incorrect, as the redox potentials of A_1 and F_X might be lowered differently due to the electrostatic interactions with reduced F_A and F_B, so that the free energy change for ET from A_1 to F_X might be modified.

Whichever of the homogeneous models is considered, the k_1/k_{-1} ratio is found to be between 0.75 and 3.2. These ratios correspond to a difference between the redox potentials of A_1 and F_X between 7 and −30 mV. With such small differences in the redox potentials, the Franck–Condon factors for ET from A_1 to F_X are expected to be small and hence the electronic factor governing this process has to be large in order to explain the high ET rate. This in turn would mean that the distance separating A_1 and F_X is rather small. One may try to estimate this distance by applying an empirical relation for the rate of intraprotein ET, which has been developed by Moser and Dutton (1992) mainly on the basis of ET measurements in purple bacterial reaction centers (Moser et al., 1992, and references therein):

$$\log k_{et} = 15 - 0.6R - 3.1(-\Delta G^\circ - \lambda)^2/\lambda \qquad (1)$$

where k_{et} is the ET transfer rate in s^{-1}, R is the edge-to-edge distance (in Å) between the reactants (measured between the center of the edge atom of the donor and the center of the edge atom of the acceptor), ΔG° is the standard Gibbs free energy of reaction in eV, and λ is the reorganization energy in eV. In the present case where $|\Delta G^\circ| << \lambda$ (see below), the preceding formula reduces to

$$\log k_{et} = 15 - 0.6R - 3.1\,\lambda \qquad (2)$$

For the reorganization energy, we follow the treatment given by Krishtalik (1989), who neglects the intramolecular reorganization energy (due to changes in the bond lengths and angles of the reactants); λ is hence identified with the reorganization energy of the medium, λ_s, expressed in analogy to a relation derived by Marcus [see, e.g., Marcus and Sutin (1985) for a review] as

$$\lambda_s = e^2 C_{eff}(1/(2r_{eff1}) + 1/(2r_{eff2}) - K/R') \qquad (3)$$

Here, e is the charge being transferred, r_{eff1} and r_{eff2} are effective radii of the reactants, and R' is the distance between their centers; C_{eff} takes into account the dielectric properties of the medium (C_{eff} increases with increasing polarity) and is estimated to be approximately 0.15 in proteins. The coefficient K, which depends slightly on the relative orientation of the partners, is approximated by 1. With this approximation, and assuming that one elementary charge is transferred, eq 3 becomes

$$\lambda_s = 14.4 C_{eff}(1/(2r_{eff1}) + 1/(2r_{eff2}) - 1/R') \qquad (4)$$

with the distances in Å and λ_s in eV. As effective radii, we use 2.84 and 4.86 Å for A_1 and F_X, respectively; the former value is the one calculated for menaquinone (Krishtalik, 1989), whereas the latter value was estimated by us using the structure of the [4Fe-4S] clusters in the ferredoxin from *Peptococcus aerogenes* (Adman et al., 1976) as an approximation for F_X. The average distances from the center of the cubane-like structure to the center of the sulfur atoms of the cluster and the cysteines, are 2.15 and 3.87 Å, respectively. The effective radius of F_X was taken as the average of these two distances plus the van der Waals radius of the sulfur atom. With these assumptions, eq 3 yields a reorganization energy between 320 and 600 mV, if the center-to-center distance, R', is varied between 7.7 Å (corresponding approximately to van der Waals contact between A_1 and F_X) and infinity. Thus, neglecting ΔG° against λ is well justified in our case.

Equations 2 and 4 can be related to one another using the approximations $\lambda = \lambda_s$ and $R' = R + r_{eff1} + r_{eff2} - 3.6$ Å (3.6 Å approximates the edge-to-edge distance at van der Waals contact). Thus one can estimate the distance and the reorganization energy which yield a given ET rate with $C_{eff} = 0.15$. The observed rate constant $k_{et} \approx 1.5 \times 10^7\ s^{-1}$ is obtained for an edge-to-edge distance of about 10.7 Å between A_1 and F_X, the reorganization energy being about 460 mV. Apart from the approximative character of eq 1 [the observed rates used by Moser and Dutton (1992) to establish eq 1 scatter by a factor of about 10 around the rates predicted by this equation], the most important uncertainties and systematic errors in this estimation are as follows.

(i) The choice of $C_{eff} = 0.15$. Using this value, Krishtalik (1989) could reproduce the reorganization energies of the primary ET reactions in purple bacterial reaction centers obtained by microscopic calculations (Creighton et al., 1988). As, however, F_X is located at the interface between the two polypeptides PSI-A and PSI-B [see, e.g., Golbeck and Bryant (1991)] in a rather hydrophilic environment, C_{eff} for ET from A_1^- to F_X may well be larger than for the primary ET reactions in purple bacteria. With an increased value of C_{eff}, the above estimation would yield a higher reorganization energy and a smaller distance between A_1 and F_X.

(ii) Neglect of the intramolecular reorganization energy. This leeds necessarily to some overestimation of the distance between A_1 and F_X.

(iii) The last term of eq 1 [$3.1(-\Delta G^\circ - \lambda)^2/\lambda$] may not hold for ET from A_1^- to F_X. In fact, this last expression implies a rather high characteristic frequency of the vibrations coupled to the ET ($\hbar\omega = 70$ meV; Moser & Dutton, 1992) so that $\hbar\omega$

Table II: Calculated Rate Constants and Kinetics for PSI-β Particles, Related to the Schemes in Figure 5

	rate constants modeling observed kinetics under moderate redox conditions[a] (F_A,F_B) (10^6 s^{-1})				prediction for A_1^- reoxidation under highly reducing conditions[b] (F_A^-,F_B^-), fastest component	
	k_1	k_{-1}	k_2	k_3	$t_{1/2}$ (ns)	proportion of total A_1^- reoxidation (%)
model 1	19.7	6.2	0	6.5	27	76
model 2	9.5	12.7	10.1	0	31	43
model 1-2[c]	15.0	8.1	4.6	4.6	30	65

[a] Each set of (k_1, k_{-1}, k_2, k_3) values gives biphasic A_1^- reoxidation with $t_{1/2}$ value of 25 and 150 ns and relative amplitudes of 65% and 35%, respectively. [b] Calculated with $k_2 = k_3 = 0$ and k_1 and k_{-1} values as given in the table for moderate redox conditions. [c] With the additional constraint $k_2 = k_3$.

largely exceeds kT even at room temperature and k_{et} becomes nearly temperature independent even for $-\Delta G^\circ \neq \lambda$. With lower values of the characteristic frequency (or stated otherwise, if the role of high-frequency vibrational modes is relatively smaller than is assumed by eq 1), k_{et} should become more temperature dependent (i.e., a thermally activated reaction) and, for a given temperature, slower than with the higher characteristic frequency (except for the special case $-\Delta G^\circ \approx \lambda$). The low efficiency of ET to the iron–sulfur centers in PSI at low temperature (Sétif et al., 1984) indicates that ET from A_1^- to F_X may be an activated reaction. If this would be confirmed (measurements in preparation), the distance between A_1 and F_X would have been overestimated by using eq 1. From these considerations, we conclude that $R = 10.7$ Å as estimated above constitutes an upper limit for the edge-to-edge distance between A_1 and F_X which would allow an ET rate of 1.5×10^7 s^{-1} with a negligible change in free energy.

With respect to the different kinetic behaviors of the different PSI preparations, it is important to note that the spectrum of the sum of the two fast phases observed in spinach PSI-β particles is fairly similar to the spectrum of the 200-ns phase observed previously (Brettel, 1988) in *Synechococcus* PSI particles (compare the two curves in the top panel of Figure 3). Except for a change in the amplitude and the wavelength of the maximum of a negative peak at 450–460 nm, the essential features of both spectra are identical. Furthermore, the spectra taken 5 ns after the flash (Figure 2, crosses and solid line) and 1.6 μs after the flash (Figure 2, squares and broken line) are, except for smaller positive absorbance changes around 450 nm, very close to the corresponding spectra in *Synechococcus* (Brettel, 1988). This suggests that both the initial (at 5 ns) and final states (at 1.6 μs) are identical in both preparations and in turn would imply that (F_A,F_B) is reduced during the 200-ns phase in the cyanobacterial preparation, practically concomitant with the reoxidation of A_1^-. This could be explained (a) by direct ET from A_1^- to (F_A,F_B) with $t_{1/2} \approx 200$ ns or (b) by sequential ET via F_X (model 1), provided that the second step is significantly faster than 200 ns ($k_3 \geq 10^7$ s^{-1}). Explanation a would imply that the ET pathway is rather different in the two preparations, whereas with explanation b, less dramatic differences in the rate constants would be sufficient. Our present experimental data do not allow a decision between these two explanations. It may be useful, however, to check whether an ET rate $k_3 \geq 10^7$ s^{-1} would be compatible with the distances between the iron–sulfur centers which were determined recently from X-ray structure analysis of PSI crystals from *Synechococcus* sp. (Krauss et al., 1992). According to the latter study, the center-to-center distances, R', between F_X and the other two iron–sulfur centers are 15 and 22 Å, but a distinction between F_A and F_B was not possible. We will refer to the center which is closer to F_X as F_I and to the other center as F_{II}. The edge-to-edge distances, R, which also depend on the (as yet unknown) relative orientation of the centers, should be between 7.3 and 10.7 Å and between 14.3 and 17.7 Å for F_X–F_I and F_X–F_{II}, respectively. To estimate the reaction free energies, ΔG°, for ET from F_X to F_A and F_B, we use the following ranges of midpoint potentials: –730 to –610 mV for F_X (Ke et al., 1977; Chamorovsky & Cammack, 1982; Parrett et al., 1989) and –600 to –510 mV for (F_A,F_B) (Ke et al., 1973; Evans et al., 1974; Evans & Heathcote, 1980). Hence, ΔG° should be between –10 and –220 meV for both reactions. Using again the approach of Krishtalik (see above) for the reorganization energies with $C_{eff} = 0.15$ and $r_{eff} = 4.86$ Å for all three iron–sulfur centers and eq 1 for the ET rates, one obtains rates between 5.1×10^7 and 3.6×10^{10} s^{-1} for ET from F_X to F_I and between 2.3×10^3 and 1.9×10^6 s^{-1} for ET from F_X to F_{II}. For the same reasons as outlined above for ET from A_1 to F_X, the approach which we used likely leads to an overestimation of the ET rates between the three iron–sulfur centers, so that the real ET can hardly be faster than the higher rates evaluated above but may be even slower than the lower values. Therefore, the rates of direct ET from F_X to F_{II} (22 Å apart) should be well below 10^7 s^{-1}; for ET from F_X to F_I (15 Å apart), however, it can only be stated that our estimation does not exclude a rate $k_3 \geq 10^7$ s^{-1}, as required for explanation b.

Although we do not yet fully understand the different kinetic behavior of the PSI particles from the cyanobacteria *Synechococcus* and *Synechocystis* and the PSI-β preparation from spinach, it is important to note that other PSI preparations from spinach, which were subjected to less harsh treatments, show kinetics which are closer to those of the cyanobacterial preparations (see Table I). Furthermore, time-resolved EPR measurements on chloroplasts from spinach showed spin-polarized spectra and kinetics very similar to those of PSI particles from *Synechococcus* (Bock et al., 1989). Hence, the different kinetic behavior of the PSI preparations investigated in the present paper may rather be related to the different treatments during extraction and purification than to intrinsic differences between cyanobacteria and higher plants. One can easily imagine that harsh preparation procedures may induce structural changes of the PSI complex, especially in those regions which are most exposed to the aqueous phase. If, for instance, the distance between two cofactors is decreased (increased) by 1 Å, the ET rate is expected to increase (decrease) by a factor 4 (eq 1). Modifications of the hydrogen bonds to the iron–sulfur clusters may appreciably affect their redox potentials (Backes et al., 1991; Langen et al., 1992) and hence the free energies and rates of ET reactions. Structural changes may also affect the vibrational modes coupled to the ET. As another possibly important factor, we would like to mention changes of the accessibility of the cofactors to the aqueous phase. Because of the much higher dielectric constant of water ($\epsilon_r \approx 80$) compared to proteins ($\epsilon_r \approx 4$), proximity of water should provide a relative stabilization of charged components. Thus,

the midpoint potentials for the reduction of A_1 and of the three iron–sulfur centers are likely to increase with closer proximity of the aqueous phase [cf. Langen et al. (1992) for the case of some iron–sulfur centers]. The extent of the potential shift may vary between these acceptors, depending on details of the PSI complex topology, so that the reaction free energies and the rates of some ET steps may be affected by treatments which change the accessibility to the aqueous phase. On the other hand, closer proximity of the aqueous phase will generally increase the reorganization energies and hence decrease the ET rate. Thus, several essential parameters which enter into the theoretical description of ET rates, namely, distance, reaction free energy, reorganization energy, and the vibrational frequencies coupled to the ET, may well be modified by harsh treatments during the preparation of PSI particles. More experimental data are required, however, to relate the observed differences in the ET kinetics to specific modifications of the PSI complex.

ACKNOWLEDGMENT

We thank Dr. Hervé Bottin for the preparation of PSI particles from *Synechocystis* 6803, Dr. Peter Bogdanoff for the preparation of spinach YEDA press PSI particles, and Professor H. T. Witt for sending us a preprint of his recent work.

REFERENCES

Adman, E. T., Sieker, L. C., & Jensen, L. H. (1976) *J. Biol. Chem. 251,* 3801–3806.

Backes, G., Mino, Y., Loehr, T. M., Meyer, T. E., Cusanovich, M. A., Sweeney, W. V., Adman, E. T., & Sanders-Loehr, J. (1991) *J. Am. Chem. Soc. 113,* 2055–2064.

Biggins, J., & Mathis, P. (1988) *Biochemistry 27,* 1494–1500.

Boardman, N. K. (1971) in *Methods in Enzymology* (San Pietro, A., Ed.) Vol. 23, Part A, pp 268–276, Academic Press, New York.

Bock, C. H., van der Est, A. J., Brettel, K., & Stehlik, D. (1989) *FEBS Lett. 247,* 91–96.

Bottin, H., & Sétif, P. (1991) *Biochim. Biophys. Acta* 1057, 331–336.

Brettel, K. (1988) *FEBS Lett. 239,* 93–98.

Brettel, K. (1989) *Biochim. Biophys. Acta 976,* 246–249.

Brettel, K., Sétif, P., & Mathis, P. (1986) *FEBS Lett. 203,* 220–224.

Chamorovsky, S. K., & Cammack, R. (1982) *Photobiochem. Photobiophys. 4,* 195–200.

Creighton, S., Hwang, J. K., Warshel, A., Parson, W. W., & Norris, J. (1988) *Biochemistry 27,* 774–781.

Evans, M. C. W., & Heathcote, P. (1980) *Biochim. Biophys. Acta 590,* 89–96.

Evans, M. C. W., Reeves, S. G., & Cammack, R. (1974) *FEBS Lett. 49,* 111–114.

Evans, M. C. W., Sihra, C. K., Bolton, J. R., & Cammack, R. (1975) *Nature 259,* 668–670.

Gerken, S., Brettel, K., Schlodder, E., & Witt, H. T. (1987) *FEBS Lett. 223,* 376–380.

Golbeck, J. H., & Cornelius, J. M. (1986) *Biochim. Biophys. Acta 849,* 16–24.

Golbeck, J. H., & Bryant, D. A. (1991) in *Current Topics in Bioenergetics* (Govindjee, Ed.) pp 83–177, Academic Press, London.

Itoh, S., & Iwaki, M. (1989) *FEBS Lett. 243,* 47–52.

Ke, B. (1972) *Arch. Biochem. Biophys.* 152, 70–77.

Ke, B. (1973) *Biochim. Biophys. Acta 301,* 1–33.

Ke, B., Hansen, R.E., & Beinert, H. (1973) *Proc. Natl. Acad. Sci. U.S.A. 70,* 2941–2945.

Ke, B., Dolan, E., Sugahara, K., Hawkridge, F. M., Demeter, S., & Shaw, E. R. (1977) in *Special Issue on Photosynthetic Organelles, Plant Cell Physiol.* 3, 187–199.

Krauss, N., Hinrichs, W., Witt, I., Fromme, P., Pritzkow, W., Dauter, Z., Betzel, C., Wilson, K. S., Witt, H. T., & Saenger, W. (1993) *Nature 361,* 326–330.

Krishtalik, L. I. (1989) *Biochim. Biophys. Acta 977,* 200–206.

Lagoutte, B., Sétif, P., & Duranton, J. (1984) *FEBS Lett. 174,* 24–29.

Langen, R., Jensen, G. M., Jacob, U., Stephens, P. J., & Warshel, A. (1992) *J. Biol. Chem. 267,* 25625–25627.

Marcus, R. A., & Sutin, N. (1985) *Biochim. Biophys. Acta 811,* 265–322.

Mathis, P., & Sétif, P. (1988) *FEBS Lett. 237,* 65–68.

McDermott, A. E., Yachandra, V. K., Guiles, R. D., Sauer, K., Klein, M., Parrett, K., & Golbeck, J. H. (1989) *Biochemistry 28,* 8056–8059.

Moser, C. C., & Dutton, P. L. (1992) *Biochim. Biophys. Acta 1101,* 171–176.

Moser, C. C., Keske, J. M., Warncke, K., Farid, R. S., & Dutton, P. L. (1992) *Nature 355,* 796–802.

Parrett, K. G., Mehari, T., Warren, P., & Golbeck, J. H. (1989) *Biochim. Biophys. Acta 973,* 324–332.

Petrouleas, V., Brand, J. J., Parrett, K. V., & Golbeck, J. H. (1989) *Biochemistry 28,* 2980–2983.

Picaud, A., Acker, S., & Duranton, J. (1982) *Photosynth. Res. 3,* 203–213.

Rustandi, R. R., Snyder, S. W., Biggins, J., Norris, J. R., & Thurnauer, M. C. (1992) *Biochim. Biophys. Acta 1101,* 311–320.

Rutherford, A. W., & Heathcote, P. (1984) *Photosynth. Res. 6,* 295–316.

Sauer, K., Mathis, P., Acker, S., & Van Best, J. A. (1978) *Biochim. Biophys. Acta 503,* 120–134.

Sétif, P. (1992) in *The Photosystems: Structure, Function and Molecular Biology* (Barber, J., Ed.) pp 471–499, Elsevier, Amsterdam.

Sétif, P., & Bottin, H. (1989) *Biochemistry 28,* 2689–2697.

Sétif, P., Mathis, P., & Vänngård, T. (1984) *Biochim. Biophys. Acta 767,* 404–414.

Sétif, P., Ikegami, I., & Biggins, J. (1987) *Biochim. Biophys. Acta 894,* 146–156.

Vernon, L. P. (1971) in *Methods in Enzymology* (San Pietro, A., Ed.) Vol. 23, Part A, pp 268–276, Academic Press, New York.